THE CHEMICAL RECORD

Ultrafast Dynamics of Myoglobin Probed by Time-Resolved Resonance Raman Spectroscopy

YASUHISA MIZUTANI,[1] TEIZO KITAGAWA[2]
[1]Institute for Molecular Science, Okazaki National Research Institutes, Myodaiji, Okazaki 444-8585, Japan
[2]Center for Integrative Bioscience, Okazaki National Research Institutes, Myodaiji, Okazaki 444-8585, Japan

Received 12 October 2000; accepted 20 November 2000

ABSTRACT: Recent experimental work carried out in this laboratory on the ultrafast dynamics of myoglobin (Mb) is summarized with a stress on structural and vibrational energy relaxation. Studies on the structural relaxation of Mb following CO photolysis revealed that the structural change of heme itself, caused by CO photodissociation, is completed within the instrumental response time of the time-resolved resonance Raman apparatus used (~2 ps). In contrast, changes in the intensity and frequency of the iron-histidine (Fe-His) stretching mode upon dissociation of the trans ligand were found to occur in the picosecond regime. The Fe-His band is absent for the CO-bound form, and its appearance upon photodissociation was not instantaneous, in contrast with that observed in the vibrational modes of heme, suggesting appreciable time evolution of the Fe displacement from the heme plane. The band position of the Fe-His stretching mode changed with a time constant of about 100 ps, indicating that tertiary structural changes of the protein occurred in a 100-ps range. Temporal changes of the anti-Stokes Raman intensity of the ν_4 and ν_7 bands demonstrated immediate generation of vibrationally excited heme upon the photodissociation and decay of the excited populations, whose time constants were 1.1 ± 0.6 and 1.9 ± 0.6 ps, respectively. In addition, the development of the time-resolved resonance Raman apparatus and prospects in this research field are described. © 2001 The Japan Chemical Journal Forum and John Wiley & Sons, Inc. Chem Rec 1:258–275, 2001

Key words: protein dynamics; vibrational energy relaxation; time-resolved vibrational spectroscopy; ultrafast spectroscopy; myoglobin

Introduction

Biological Relevance of Ultrafast Protein Dynamics

Protein dynamics spans over a wide range of time scales.[1,2] To answer questions on protein dynamics, we need the concatenation of experimental results recorded over many orders of magnitude of time. In this regard, it is important that a single experimental technique can examine protein structures evolving from the earliest moments, such as the picosecond regime, toward time scales that are highly relevant to biological func-

▸ *Correspondence to:* T. Kitagawa (E-mail: **teizo@ims.ac.jp**).

Contract grant sponsor: Ministry of Education, Science, Sports and Culture, Japan; contract grant number: 12045264 (T.K.).
Contract grant sponsor: Japan Society for the Promotion of Science; contract grant number: 11740339 (Y.M.).

The Chemical Record, Vol. 1, 258–275 (2001)

tions, such as the microsecond or millisecond regimes. One might ask whether ultrafast spectroscopy can contribute anything to the understanding of protein systems. There are some good reasons for us to believe that the answer is positive. One method for studying the dynamic motions of proteins is to pursue the ensuing relaxation after shifting a protein from equilibrium. If we use short pulses to initiate a very rapid photoreaction at an active site immediately after the start of a reaction, the result is a metastable structure with an active site that is different, but the tertiary and quaternary structures of the protein are similar to the original state. The surrounding "protein solvent" is now the structural variable. A short probe pulse following the initiating pulse provides direct information on the relaxation of this metastable form into the equilibrium protein structure. In this way, the quickest responses of proteins can be monitored by ultrafast spectroscopy.[3] Another feature to be noted about ultrafast spectroscopy is the possibility of studying energy dissipation in proteins, which is very important in order to understand reactions in proteins. In general, energy dissipation occurs in the sub-picosecond to picosecond regime in the condensed phases.[4–6] Ultrafast spectroscopy is required in order to study how the deposited energy dissipates in proteins. In addition to such relaxation processes, there are conformational fluctuations around the equilibrium points. The tertiary structure is undergoing fluctuations on a time scale of hindered molecular rotations. These motions can also be studied by various ultrafast spectroscopic techniques, including photon echo[7–9] and hole-burning spectroscopy.[8,10]

Myoglobin Corresponds to "Hydrogen Molecule in Chemistry"

Protein dynamics are intimately connected to the structure/function relationship of biological systems. In numerous biological processes, the ensuing protein structural changes accompanying a reaction at a specific site must spatially extend to the mesoscopic dimensions of the protein to achieve a biological function. The molecular mechanism of cooperativity in

Yasuhisa Mizutani was born in Mie, Japan, in 1964. He earned his Bachelor of Engineering and Master of Engineering degrees in 1987 and 1989, respectively, from Kyoto University, working with Professor Koichiro Nakanishi. He received his PhD degree from the Graduate University for Advanced Studies in 1992 under the supervision of Professor Teizo Kitagawa. After that, he did postdoctoral work at the Institute for Molecular Science and at the University of Pennsylvania, where he worked as a postdoctoral fellow for Professor Robin M. Hochstrasser. In 1994, he joined the faculty at the Institute for Molecular Science, as a research associate. His research interests include dynamical aspects of chemical reaction in liquids and proteins and spectroscopic approaches to them. ■

Teizo Kitagawa was born in Kyoto, Japan in 1940. He graduated from the engineering department of Osaka University in 1963, and received his Master of Science and PhD degrees in 1965 and 1969, respectively, from Osaka University, under the supervision of Professor Tatsuo Miyazawa. He became a research associate of the Institute for Protein Research, Osaka University, in 1966, an associate professor at the Medical School of Osaka University in 1980, and a full professor at the Institute for Molecular Science in 1983. During his research associate period, he studied vibrational spectra of polymer crystals and related solid state properties, including neutron inelastic scattering, and he worked as a postdoctoral fellow for Professor Bryce L. Crawford at the University of Minnesota, studying liquid dynamics using ATR spectroscopy. Since coming back from the USA, he has studied the dynamic structure-function relationship of proteins using vibrational spectroscopy. ■

oxygen binding of hemoglobin (Hb) is one of the classical problems in this aspect.[11] The large-amplitude motions at the quaternary level, which form a communication link at the subunit interface, are driven by changes in the tertiary structure upon ligation. In this respect, myoglobin (Mb) serves as a model system for the tertiary relaxation processes. Structurally very similar to a subunit of Hb, Mb is involved in oxygen storage in muscles. Twenty years after a pioneering microsecond flash photolysis study by Gibson,[12] the first ultrafast optical spectra of hemeproteins were reported.[13] Ultrafast optical absorption studies[13,14] revealed that the excited-state surface of the ligated heme is dissociative, so it is possible to photoinitiate a structural change from the ligated form to the deligated form within 50 fs with quantum yield of nearly unity. By using CO as the ligand rather than O_2, it is possible to avoid the geminate recombination processes complicating the reaction dynamics in the picosecond regime.[15] Thus, the carbonmonoxy myoglobin (MbCO) system is unique in that it gives access to the full range of protein relaxation processes to a single perturbation (ligand dissociation) without complicated side reactions and associated population dynamics. These features of MbCO make it possible to trigger optically the structural changes of a protein and follow the structural relaxation using optical probes that are sensitive to different aspects of the protein's motion. For this reason, an enormous body of work has been accumulated about Mb relaxation processes, helping to establish general principles related to protein dynamics.

The three-dimensional structure of the deligated form of Mb (deoxyMb)[16] is shown schematically in Figure 1(A), in which the arrow points to the heme prosthetic group. The heme is an iron-protoporphyrin IX (Fe^{II}PPIX), in which the Fe^{II} ion is bound to the proximal histidine (His) as the only covalent link to the protein in Mb. The heme iron binds diatomic molecules, such as NO, CO, and O_2, at the opposite side of the proximal His. X-ray crystallography provided extensive information about the endpoint equilibrium structures, as schematically shown in Figure 1(B). The magnitude of atomic displacements at the heme site that must occur on ligand binding and release is estimated by examining the structures containing the heme with and without bound ligands. The ligated heme has a planar structure in which the low-spin iron atom is in the porphyrin plane. For MbCO, the core size, that is, the distance between the pyrrole nitrogen atoms and the heme center, is 2.005Å.[16] Upon ligand dissociation, the iron atom is converted from low to high spin (S=0→S=2) and moves out of the porphyrin plane by about 0.3Å. Concomitantly, the porphyrin core size expands to 2.057Å.

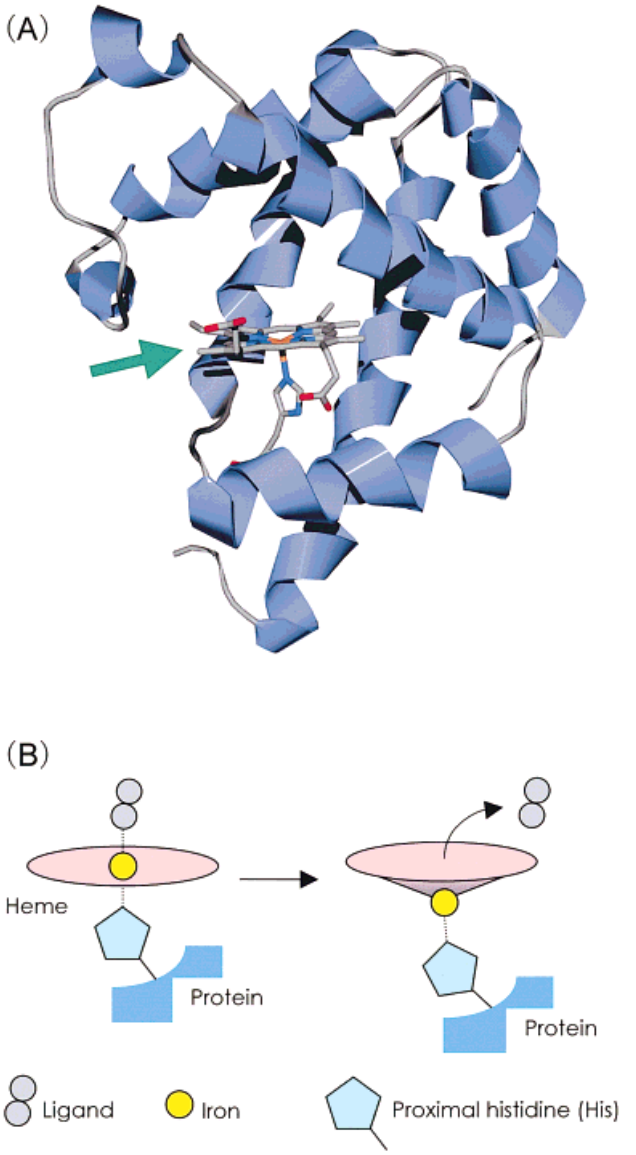

Fig. 1. (A) Three-dimensional structure of the deoxy form of Mb based on the PDB structure (identification code, 1BZP).[16] (B) Heme structure of the ligated form (left) and of the deoxy form (right). The doming of the heme ring, out-of-plane displacement of the iron, and tilting of the proximal histidine are key motions. These motions ultimately couple to the helical sections of globin and induce a change in the tertiary structure.

Choice of the Method to Monitor Ultrafast Protein Dynamics

Some of the faster processes in protein motions involve relatively small alterations in the overall structure. Therefore, the probes used to examine them must be sensitive to subtle changes in the protein structure. For this reason, we decided to use the vibrational spectroscopic method, which is sufficiently structure sensitive at chemical-bond resolution so as to allow identification of any ultrafast steps in protein dynamics. Among several techniques to detect vibrational spectra, we used Raman spectroscopy for the following reasons. Firstly, water interferes less with Raman spectra compared to infrared spectra. This is an important advantage for studies of protein solutions, which have water as a

solvent. Secondly, resonance Raman effects offer the advantages of high selectivity and increased sensitivity when the wavelength of the probe light is tuned to an electronic transition of the intermediate of interest. At the same time, the selectivity can be utilized to probe only the prosthetic groups of proteins, which often serve as active sites. For example, we can monitor only the structure of the heme in the protein resulting from the resonance effect.[17] Both time-resolved resonance Raman (TR^3) and infrared spectroscopy provide inherently ultrafast time resolution and, thus, detailed structural information. In infrared spectroscopy, high resolutions in frequency and time can be obtained simultaneously if the coherent interaction between an ultrashort probing pulse and a sample is carefully considered,[18,19] because frequency selection by a spectrometer can be performed after the light pulse interacts with the molecule. However, it is still a hard task to measure femtosecond or picosecond time-resolved IR spectra in a wide frequency range (300 to 3000 cm^{-1}) because of interference by solvent bands and difficulties in the generation of broad infrared pulses and their multichannel detection, although development of the transient femtosecond IR technique is progressing.[20–24] Comparatively, in TR^3 spectroscopy, subpicosecond time resolution is not compatible with a high resolution in frequency because the resolutions are achieved during the same interaction between the light pulse and molecule. Nevertheless, this technique has an advantage in that many vibrational transitions in a wide frequency range can be simultaneously observed with a single frequency of probe light. Moreover, time-resolved anti-Stokes Raman spectroscopy is selective for vibrationally excited modes, and it is therefore a powerful method for measuring vibrational energy relaxation.[25–27] The high repetition rate of modern Ti:sapphire laser systems enables sufficiently high signal-to-noise ratios, which in turn enables the application of ultrafast TR^3 experiments in protein systems, as described in the following section.

Mb as a Solution Model: Heme Solute in Protein Solvent

Although a heme and a protein constitute a single molecule, the heme prosthetic group is relatively isolated from the protein and approximates to a heme in a solution. The heme is linked covalently to the surrounding globin through the proximal His. Motion along the Fe-His coordinate is orthogonal and, to a first approximation, decoupled from the vibrational modes of the porphyrin ring. The heme is maintained in a cavity by approximately 90 van der Waals contacts with the protein.[28] Therefore, the heme can be regarded as a solute molecule dissolved in a "protein solvent." For example, the protein structure is perturbed by a structural change in the heme site upon CO photolysis. The accompanied structural relaxation is analogous to the solvation dynamics studied by dynamic Stokes shift of fluorescent molecules in polar solvents.[29] Therefore, for Mb, the dynamic aspects of proteins, including structural and energy relaxation, and conformational fluctuations, can be understood from the point of view of how the protein acts as a medium for chemical reactions at the active site (i.e., the heme site).

In this article, we summarize our recent experimental work on the ultrafast dynamics of Mb. Our development of a time-resolved resonance Raman apparatus is described in the next section. Studies on the structural and vibrational energy relaxation of Mb following CO photolysis are also explained. A summary and perspectives are given in the last section.

Picosecond Time-Resolved Resonance Raman Spectrometer[30,31]

Picosecond time-resolved resonance Raman (ps-TR^3) spectroscopy is a promising technique to investigate the ultrafast structural changes of molecules.[32] Nevertheless, ps-TR^3 spectroscopy is not implemented as widely as nanosecond TR^3 spectroscopy because of practical limitations. The most crucial factor is a lack of a light source that fulfills the requirements for small timing jitters, appropriate repetition rates, and the wavelength tunability of pulses applicable to ps-TR^3 spectroscopy, which requires two beams: a pump beam to photoexcite molecules of interest and a probe beam to monitor the subsequent changes occurring in the excited or reacted molecules. To obtain the TR^3 spectra of a wide variety of molecules with high S/N ratios within a reasonable measuring time, it is quite important to use two independently tunable light sources with a high repetition rate for the pump and probe beams. Repetition rates in the kilohertz range are desirable for practical purposes, but so far, no one has succeeded in observing ps-TR^3 spectra with a widely tunable pulse source at kilohertz repetitions. We constructed an apparatus consisting of widely tunable light sources for ps-TR^3 spectroscopy using a 1-kHz picosecond Ti:sapphire laser/regenerative amplifier system.[30]

Laser System

Figure 2 is a schematic of the apparatus. A picosecond mode-locked Ti:sapphire oscillator (Spectra-Physics, Tsunami 3950), pumped by an Ar^+ ion laser (Spectra-Physics, BeamLok 2060), produced approximately 1.5-ps pulses with a repetition of 82 MHz and an average power of about 0.7 W. The seed pulse was amplified by a regenerative amplifier (Positive Light, Spitfire) operated at 1 kHz by pumping with the 527-nm output of an intracavity frequency-doubled Nd:YLF laser. This amplification unit provides 784-nm pulses, each with an energy of about 0.8 mJ, a duration of 2.5 ps, and a spectral width of 6 cm^{-1} in a nearly TEM_{00} mode under operation at 1 kHz. The whole laser system was covered with a plastic sheet, which was equipped with dust cleaners containing high-efficiency particu-

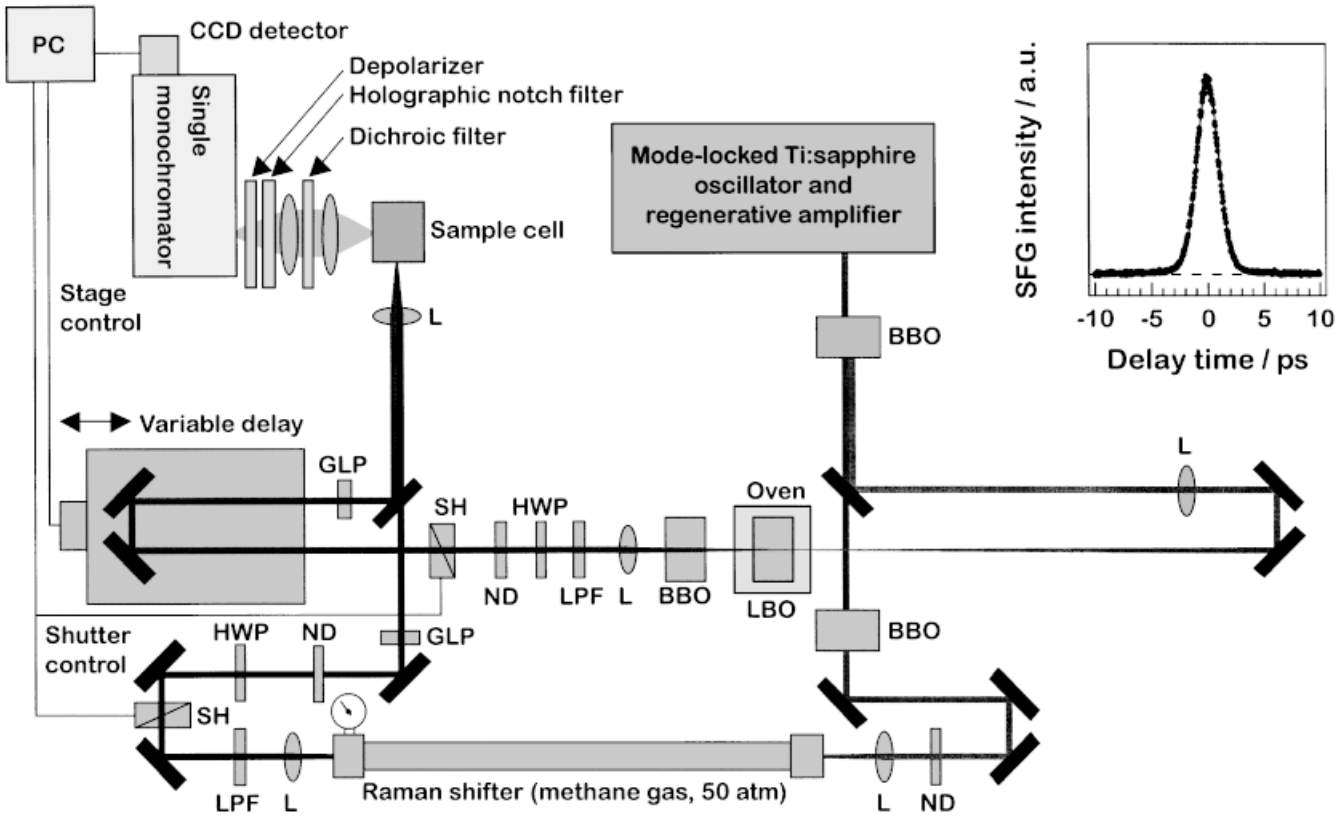

Fig. 2. ps-TR^3 apparatus: BBO = β-barium borate, GLP = Glan laser linear polarizer, HWP = half-wave plate, L = lens, LBO = lithium triborate, LPF = long wavelength pass filter, ND = neutral density filter, PC = personal computer, SH = shutter. The inset shows a cross-correlation trace (dots) of the pump and probe pulses, which was obtained using background-free sum frequency generation in a BBO crystal. The trace was best fit by a Gaussian function (solid line) to yield a width of 2.3 ps.

late air (HEPA) filters to keep the laser system free of dust. In the pump arm, a pump pulse of 540 nm was generated with a home-built optical parametric generator (OPG) and amplifier (OPA), which were pumped with the second harmonic of the 784-nm output. In the probe arm, a probe pulse of 442 nm was generated as the first Stokes stimulated Raman scattering from compressed methane gas (50 kg/cm^2) excited by the second harmonic of the 784-nm output. Components other than the first Stokes scattering were removed spectrally with a glass filter and dichroic mirrors and spatially with a Pellin-Broca prism. The energy and bandwidth of the OPG-OPA output was 30 μJ and about 3 nm, respectively. The pulses were used for the pump beam for the ps-TR^3 measurements in this work after they were attenuated to 10 μJ using a Cr-coated quartz ND filter. The energy and bandwidth of the stimulated Raman scattering was between 1.0 and 1.5 μJ and 14 cm^{-1}, respectively. The first Stokes scattering was attenuated to 0.1 μJ using the Cr-coated quartz ND filter. The pump and probe beams were made collinear and coaxial using a dichroic mirror. The polarization of the pump beam was rotated by 55° relative to that of the probe beam to minimize the effects of molecular rotations on the observed kinetics. Both beams were always monitored with photodiodes (Hamamatsu Photonics, S2387-1010R) and were found to be stable within ±10%. The inset of Figure 2 shows a cross correlation trace of the pump and probe pulses measured with a 1-mm BBO crystal, indicating a width of 2.3 ps. The 0.0 ps of delay time (uncertainty <0.2 ps) was calibrated using sum frequency mixing in the same crystal.

Data Acquisition

The sample solution was placed in a 10-mmϕ NMR tube and spun with a spinning cell device that was designed to minimize the off-center deviation during rotation.[33] The sample was spun at 3400 rpm in the spinning cell configured for 135° backscattering illumination and collection. This configuration is important to minimize the effects of molecular rotations on the observed kinetics.[34] Spherical and cylindrical lenses were used to focus the pump and probe beams on the sample. In ps-TR^3 experiments, it is very important to use weak probe power. The

probe power was empirically selected so that the sample had no anti-Stokes ν_4 band of the photoproduct in the probe-only spectrum (this is discussed elsewhere). The spectral features of photoproducts in the pump-probe spectra were also shown to be invariant to a threefold change of the probe power. The pump power was selected so that no saturation effect or spectral changes occurred by a tripling of the pump power.

The TR^3 data acquisitions were carried out as follows. In the forward scan of delay time, delay times were changed by increasing them. At each delay time, Raman signals were collected for three 20-s exposures with both the pump and probe beams present in the sample. This was followed by equivalent exposures for pump-only, probe-only, and dark measurements. Measurements in the backward scan of delay time were done using the same procedure, except for the direction of change in delay time. The transient Raman data were obtained by averaging the data for 10 entire cycles for Stokes spectra and 90 entire cycles for anti-Stokes spectra. This method enabled us to avoid the errors caused by a slow drift of laser power and to obtain quantitatively reproducible spectra from one day to the next, which was possible because of the excellent long-term stability of this laser system. The pump-only spectrum was directly subtracted from the pump-and-probe spectrum, yielding the "probe-with-photolysis" spectrum. The dark spectrum was directly subtracted from the probe-only spectrum, yielding the "probe-without-photolysis" spectrum (MbCO). The probe-without-photolysis spectrum was subtracted from the probe-with-photolysis spectrum to yield the photoproduct spectrum. The subtraction parameter was determined by subtracting the probe-without-photolysis spectrum from the probe-with-photolysis spectrum until negative features were seen at the location of prominent bands of MbCO. The subtraction parameter was then reduced until these negative peaks were just eliminated, thereby accounting for the depletion of MbCO caused by the pump pulse. The scattering intensity for the change in the optical absorption of the sample at each time point was corrected by normalizing the data to the intensity changes of the 982-cm^{-1} line of sulfate ions dissolved into the sample.

Raman scattering was collected by a doublet achromat [80-mm focal length (FL), *f*/2] and was imaged onto the 200-μm entrance slit of a single spectrometer (Spex, 500M) by a doublet achromat (200-mm FL, *f*/5). A dichroic short-pass filter was placed between the lenses to remove the scattered pump beam. A holographic notch filter (Kaiser Optical Systems, HSNF-441.6-1.0) was used to reject the unshifted scattering. A polarization scrambler was placed at the entrance slit to remove the effects of polarization on the spectrograph throughput. The spectrograph is equipped with a blazed-holographic grating (2400 grooves/mm) that enables measurements of a spectrum as wide as about 1000 cm^{-1} in the Soret region, and with a spectral slit width of approximately 8 cm^{-1}. The dispersed light was detected by a liquid nitrogen cooled CCD detector (Princeton Instruments, CCD-1100PB). Raman shifts were calibrated with cyclohexane, benzene, or carbon tetrachloride. The peak positions of Raman bands are accurate within ±2 cm^{-1}.

Structural Relaxation of Mb[35]

Raman Spectral Change of the Heme

Figure 3 shows the Stokes time-resolved resonance Raman difference spectra of photodissociated Mb for various values of delay times of the probe pulse with respect to the pump pulse. In these spectra, the contribution of unreacted species has been subtracted. The fraction of photolyzed MbCO was estimated to be 6% based on the intensity loss of the Raman bands of MbCO. The TR^3 spectrum in the 1000 to 1700-cm^{-1} region for a 1-ps delay (Fig. 3) contains only the bands arising from the in-plane vibrations of heme at 1352 (ν_4), 1560 (ν_2), and 1617 (ν_{10}) cm^{-1}.[36,37] These bands exhibited an appreciable narrowing and frequency upshift in the first few picoseconds, but no further changes occurred after that (as is discussed in the section "Vibrational Energy Relaxation"). The TR^3 spectrum for a 10-ps delay closely resembles the spectrum of deoxyMb, indicating that the photodissociated heme has relaxed to the equilibrium structure within the instrument response time (~2 ps). Most interestingly, the ν_2 band, which has a frequency that is well known to be sensitive to the core size of the porphyrin ring, appeared at a position close to that of the ν_2 band of deoxyMb. This demonstrates that expansion of the core size is instantaneous upon CO photodissociation. There is no Raman band that can be assigned to the excited electronic state. The involvement of the excited electronic state in the relaxation pathway remains a possibility, and there are reports that suggest this is likely.[38–40] However, the results in this work and in other studies[41,42] indicate that a majority of the population is directly channeled into the vibrational manifolds of the ground electronic state, and minor channels may lead to an appearance of small amounts of long-lived (ps time scale) intermediate states.[41] The intensity invariance in the spectra for delay times between 5 and 50 ps is consistent with the fact that recombination of CO to the heme takes place in the time regime of micro- to milliseconds,[43] in contrast with the cases for NO and O_2.[15] Accordingly, these results show that the heme in Mb is led to the ground electronic state and expanded to the equilibrium core size within the instrument response time.

Figure 4 shows the TR^3 spectrum in the 150 to 850-cm^{-1} region and delay of between –7 and 1000 ps. The bands at 220, 301, 369, and 671 cm^{-1} in the spectrum for a 1000-ps delay are assigned to the vibrations of the heme: ν (Fe-His),[44] γ_7,[45] $\delta(C_\beta C_c C_d)$,[45] and ν_7, respectively. The large peak at about 220 cm^{-1} is caused by the stretching mode of the covalent bond between the heme iron and the N_ε of His93, ν (Fe-His). The

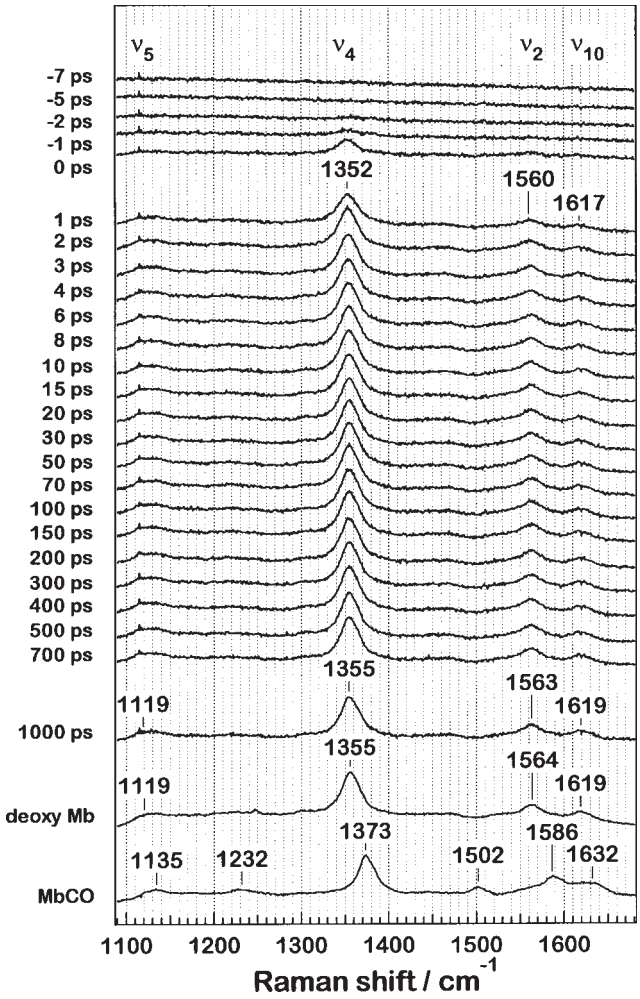

Fig. 3. TR³ Stokes spectra of photodissociated MbCO in the 1100 to 1700-cm^{-1} region. Stokes spectra of the equilibrium deoxyMb and MbCO are depicted at the bottom for comparison. Horse skeletal Mb (Sigma, M-0630) was dissolved into a buffer (50 m*M* Tris·HCl, pH 8.0) and filtrated through a 0.45-μm PTFE membrane (Millipore) to make a 300-μ*M* solution. One milliliter of the Mb solution was placed into an airtight NMR tube (10 mmϕ). The remaining oxygen in the solution was removed by more than five cycles of degassing and back-filling with CO. Finally the solution was equilibrated under 1 atm of CO. The samples were reduced with a fivefold stoichiometric amount of sodium dithionite in a small amount of solution (approximately 50 μL). The sample solution in the cell was continuously spun during the measurements to prevent multiple probing of the same portion of sample. The sample was replaced with a new one every 3 h. Sample integrity was confirmed with ultraviolet (UV)-visible absorption spectra after the TR³ measurements. The samples of deoxyMb were prepared by the same procedure as MbCO, except for back-filling with N_2 and the equilibration of the sample under 1 atm of N_2.

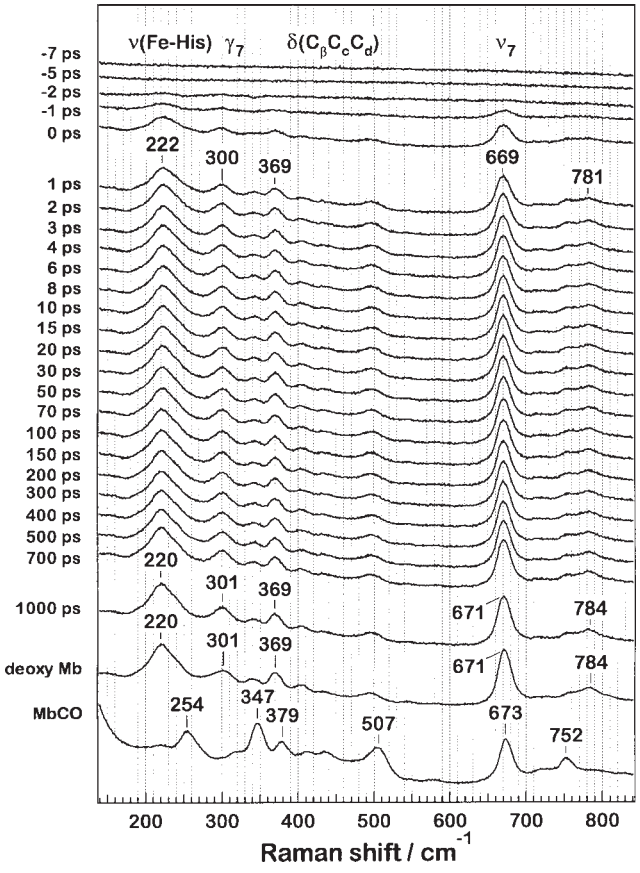

Fig. 4. TR³ Stokes spectra of photodissociated MbCO in the 150 to 850-cm^{-1} region. The Stokes spectra of the equilibrium deoxyMb and MbCO are depicted at the bottom for comparison. Experimental conditions are the same as those of Figure 3.

peak at 301 cm^{-1} is γ_7 (out-of-plane methine wagging). The peak at 369 cm^{-1} is assigned to δ ($C_\beta C_c C_d$), a mode involving deformation of the propionate methylene groups. The peak at 671 cm^{-1} is ν_7 (breathing-like mode of the porphyrin inner ring). As was observed for the spectra in the high- frequency region, RR bands exhibited appreciable frequency upshifts in the first few picoseconds, but no further large changes occurred after that.

Structural Change of the Fe-His Linkage

The iron-proximal histidine bond is the only linkage between the heme and globin, and it thus functions as the focal point for the forces driving the structural changes. In this regard, TR³ studies of the proximal His are key to elucidating the protein dynamics. The ν(Fe-His) mode is one of the most focused Raman bands in Mb and Hb, and it is known to serve as a good measure of the tertiary and quaternary structures of globin.[46,47] Recently, work on the Mb and Hb problem with the use of resonance Raman spectroscopy has made significant progress. The assignment of the Fe-His mode at around 216–220 cm^{-1} by Kitagawa and his coworkers[44,56] led to a variety of investigations involving R → T conformational changes, as well as histidine deprotonation, cryogenic, and comparative studies. To study protein relaxation, we closely examined the tem-

poral behavior of the ν(Fe-His) band in comparison with those of other heme Raman bands.

The temporal behaviors of the Raman band intensities observed for Mb are plotted in Figures 5 (ν_7 and ν_4 bands) and 6 [γ_7 and ν(Fe-His) bands]. Results from an investigation of the temporal behavior demonstrate that the band intensities of heme in-plane (ν_7 and ν_4 bands) and out-of-plane vibrations (γ_7 band) develop within the instrument response time and remain constant. In contrast, the band intensity of ν(Fe-His) shows a gradual increase up to a 20-ps delay, in addition to an instantaneous rise upon photodissociation. The fraction of the slow rise component is 8 ± 1%. Because there is no intensity change in the heme in-plane and out-of-plane vibrational modes in a time range of 3 to 50 ps, the gradual intensity increase in the ν(Fe-His) band is ascribed to the structural changes in the Fe-His linkage. The same measurements were carried out for a model system without a protein matrix, which is a 2-methylimidazole complex of iron protoporphyrin-IX, (Fe^{II}PPIX)-2MeIm, in a 0.1% CTAB (hexadecyltrimethylammonium bromide) aqueous solution. The results are shown in Figure 7. Temporal behavior similar to that for the corre-

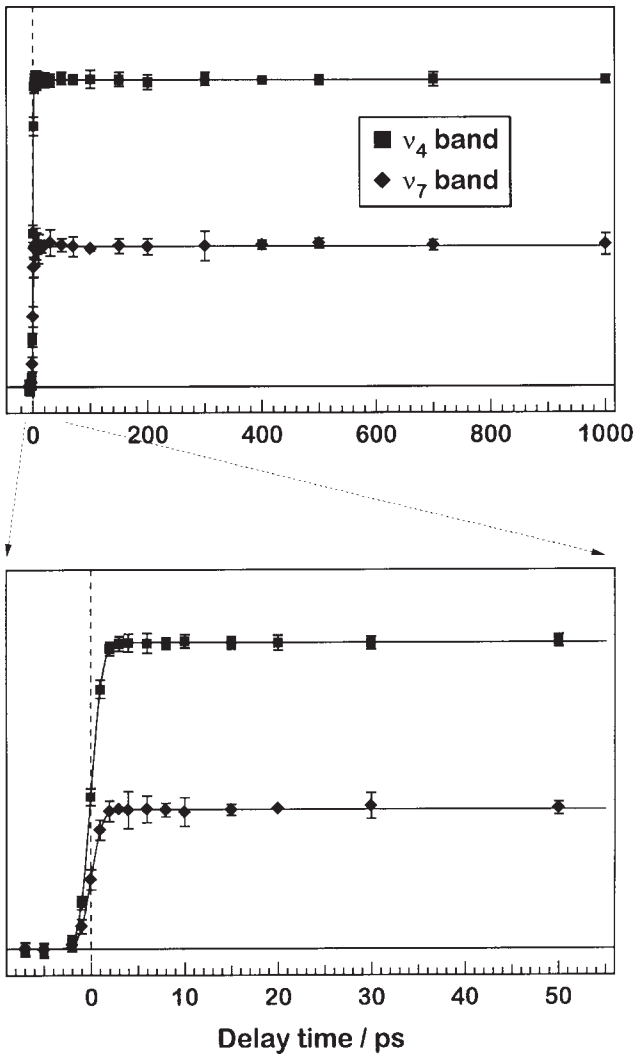

Fig. 5. Temporal change of the Raman intensity of the Stokes ν_4 (squares) and ν_7 bands (diamonds) of photodissociated MbCO. The lines are calculated for a step function (assuming an instantaneous rise and very slow decay) convoluted with a Gaussian instrument response function for which the cross correlation time is 2.3 ps. The lower panel shows a closeup of the curve in the early time region.

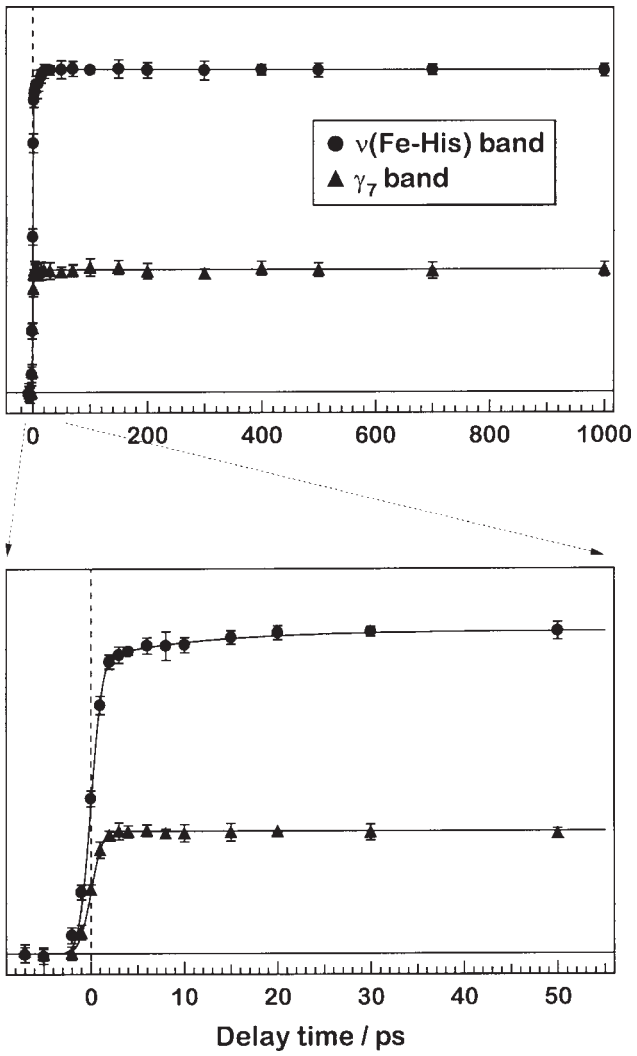

Fig. 6. Temporal change of the Raman intensity of the Stokes ν(Fe-His) (circles) and γ_7 bands (triangles) of photodissociated MbCO. The solid line for the ν(Fe-His) mode is a fit using an exponential function of the form $A[1-B\exp(-t/\tau_{rise})]$ (a rise containing instantaneous and slow phases and very slow decay) convoluted with the instrument response function, as shown in the caption of Figure 5. The line for the ν(Fe-His) mode shown in this figure was obtained with the parameters of τ_{rise} = 6.5 ± 2.5 ps and B = 0.08 ± 0.01. The solid line for the γ_7 mode is a fit using a step function convoluted with the instrument response function. The lower panel shows a closeup of the curve in the early time region.

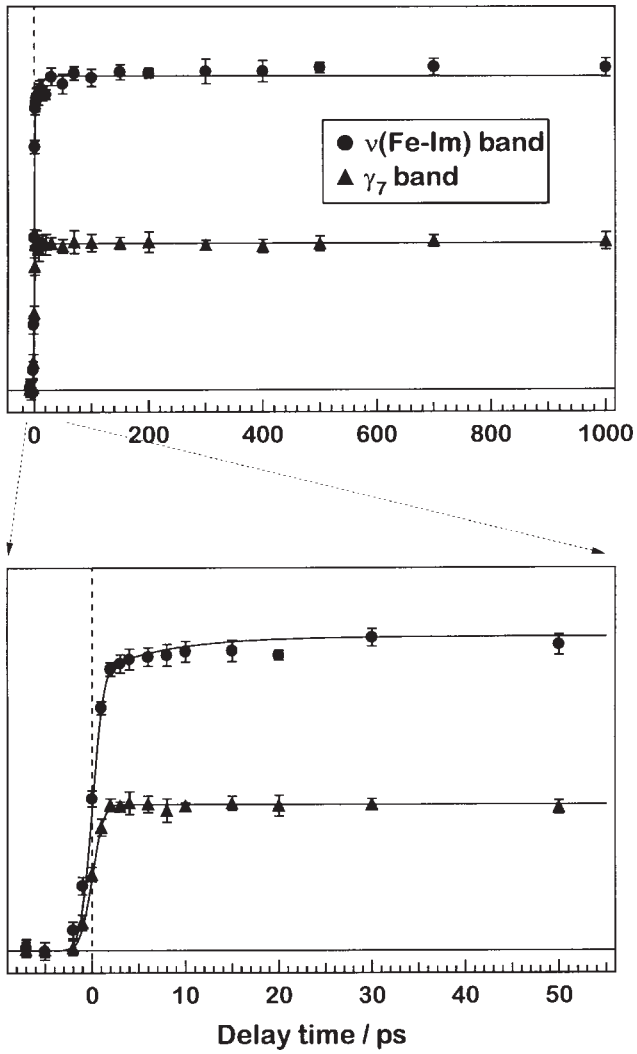

Fig. 7. Temporal change of the Raman intensity of the Stokes ν(Fe-Im) (circles) and γ_7 bands (triangles) of the photoproduct of the CO-bound (Fe^{II}PPIX)-2MeIm complex. The solid line for the ν(Fe-Im) mode is a fit using an exponential function of the form $A[1-B\exp(-t/\tau_{rise})]$ (a rise containing instantaneous and slow phases and very slow decay) convoluted with the instrument response function, as shown in the caption of Figure 5. The line for the ν(Fe-Im) mode shown in this figure was obtained with the parameters of $\tau_{rise} = 7.8 \pm 2.7$ ps and $B = 0.11 \pm 0.02$. The solid line for the γ_7 mode is a fit using a step function convoluted with the instrument response function. Hemin (Sigma, H-2250) was dissolved into buffer (50 m*M* Tris·HCl, pH 8.0) containing 0.1% CTAB and 15 m*M* 2-methylimidazole, and then filtrated through a 0.45-μm PTFE membrane (Millipore) to make a 300-μ*M* solution. The lower panel shows a closeup of the curve in the early time region. The procedure for the preparation of the CO-bound form of the complex was the same as that for MbCO.

sponding modes of Mb were observed for the ν(Fe-Im) and the heme vibrational bands of the complex, indicating that the structural change is not associated with protein relaxation and that it is a characteristic of the heme-histidine (or imidazole) unit.

To understand the intensity behavior of the Fe-His stretching mode, we followed the analysis of Bangcharoenpaurpong et al.[48] The Fe-His configuration is defined by: the out-of-plane displacement caused by ligand photodissociation (defined as the distance from the average plane of the porphyrin ring); the tilt angle of the Fe-His bond (relative to heme normal); and the azimuthal angle (about heme normal). Bangcharoenpaurpong et al. found that the Fe-His stretching vibration is relatively strongly coupled to the Soret transition.[48] Their hypothesis is that the origin of the RR intensity of the Fe-His vibrational mode results from the electronic overlap between the σ^* orbital of the Fe-His bond ($\sigma^*_{Fe\text{-}NHis}$) and the π^* orbital of the porphyrin ring (π^*_{por}) created by these structural changes. For nearly zero degree of the azimuthal angle, the orbital mixing of $\sigma^*_{Fe\text{-}NHis}$-$\pi^*_{por}$ may occur. The electron-electron repulsive interaction between the single electron in $\sigma^*_{Fe\text{-}NHis}$ and the filled π_{por} electron density on the heme nitrogens can lead to $\sigma^*_{Fe\text{-}NHis} \rightarrow \pi^*_{por}$ electron donation. The π_{por}-π^*_{por} excitation can result in direct harmonic coupling of the $Fe\text{-}N_{His}$ mode via the orbital mixing of π^*_{por} and $\sigma^*_{Fe\text{-}NHis}$ (the π_{por}-π^*_{por} transition gives rise to the Soret band). The stronger this coupling, the higher the resonance Raman intensity of the Fe-His stretching mode upon Raman excitation into the Soret band. The band intensity of the ν(Fe-His) mode increases with increasing out-of-plane displacement of iron because of the creation of an overlap between the $\sigma^*_{Fe\text{-}NHis}$ and π^*_{por} (which is zero by symmetry for the in-plane iron). Just as the azimuthal rotation affects the coupling, the tilt angle also affects it: the greater the tilt angle, the stronger the coupling. No (or only weak) coupling to the Soret transition occurs when the tilt angle is zero.

We now consider the origin of the slow phase of the ν(Fe-His) intensity change that was observed both for Mb and the model compound. A high-resolution X-ray study[16] indicated that the iron out-of-plane displacement is about 0.3Å in the deoxy structure and decreases to around 0Å upon CO binding. The difference in the tilt angle is slightly altered by CO binding: 10° in the deoxy form[49] and 0° in the CO-bound form.[50] However, the azimuthal angle remains unaltered at 19° for both the deoxy and CO-bound forms.[49,50] Accordingly, among the three factors mentioned above, the iron out-of-plane displacement and the tilt angle are possible structural parameters from which the slow phase of the ν(Fe-His) intensity change originated.

A molecular dynamics (MD) simulation by Kuczera et al.[51] pursued the time-dependent out-of-plane displacement of iron after ligand dissociation. The trajectory indicated that 80% of the out-of-plane displacement occurred within 50 fs, corresponding to the motion of the iron along the repulsive part of the iron-porphyrin potential energy surface. The results also predicted that 20% of the out-of-plane displacement of iron occurs over time scales ranging from a picosecond to tens of picoseconds. The bandshift of band III in the near IR region

observed in the ultrafast transient absorption spectra of Mb at an ambient temperature was interpreted successfully along this line.[52] A comparison of the band III shift with the trajectory of the MD simulations by Kuczera et al.[51] indicated that the temporal behaviors correlate with one another over the first 100 ps of relaxation. The temporal behaviors of ν(Fe-His) intensity resemble those of the position of band III and the out-of-plane displacement of Fe in the MD simulation. According to this, we concluded that the slow rise of ν(Fe-His) intensity primarily originates from the slow phase of the iron out-of-plane displacement. However, there are contrasting MD simulations[53,54] that indicate that complete heme doming occurs on a time scale of less than 1 picosecond. These results suggest that the slow rise of ν(Fe-His) Raman intensity must result from a change in the tilt angle. At the present stage, it is difficult to attribute the slow rise of ν(Fe-His) intensity exclusively to either structural parameter. In either case, the structural change responsible for the slow rise does not involve global conformational changes of the protein, as was similarly observed for Mb and the (Fe^{II}PPIX)-2MeIm complex.

The peak positions of the observed five bands of Mb and the (Fe^{II}PPIX)-2MeIm complex are plotted against time in Figure 8. For Mb, the ν(Fe-His) band showed a small downshift in the 100-ps time range, but the other two bands showed no shift in this range [Fig. 8(A,B)]. In contrast, neither the ν(Fe-Im) nor the γ_7 band of the (Fe^{II}PPIX)-2MeIm complex showed a frequency shift as the delay time increased [Fig. 8(C)]. Therefore, the downshift of the ν(Fe-His) band of Mb should be attributed to some change in the ligation state of the proximal His caused by a structural change of globin. The downshift of the ν(Fe-His) band of Mb can be well described by single-exponential kinetics, providing a time constant of around 100 ps, although the kinetics would involve several steps of relaxation. The protein relaxation of Mb upon CO dissociation was previously thought to complete within 30 ps because previous TR^3 measurements with a 30-ps wide pulse could not detect any frequency difference between the initial 30-ps spectrum and the equilibrium spectra.[55] However, this high-precision study revealed the presence of the relaxation process of Mb in the 100-ps time range.

Previous Raman studies on equilibrium deoxyHbs[56–58] and photoinduced ligand-free transient Hbs[59–63] have demonstrated that the frequency of the Fe-His stretching mode is responsive to a quaternary structure. In addition, studies on the transients[59–61] have revealed that this frequency is sensitive to ligand-induced changes in the tertiary structure within both the R and T quaternary states. The general trend is that the frequency of this mode increases in going from the T to the R states, and that the changes within a given quaternary structure caused by ligand binding push the frequency still higher. Picosecond studies show that the frequency in a nanosecond time scale is already fully developed within 25 ps following photolysis.[55] As

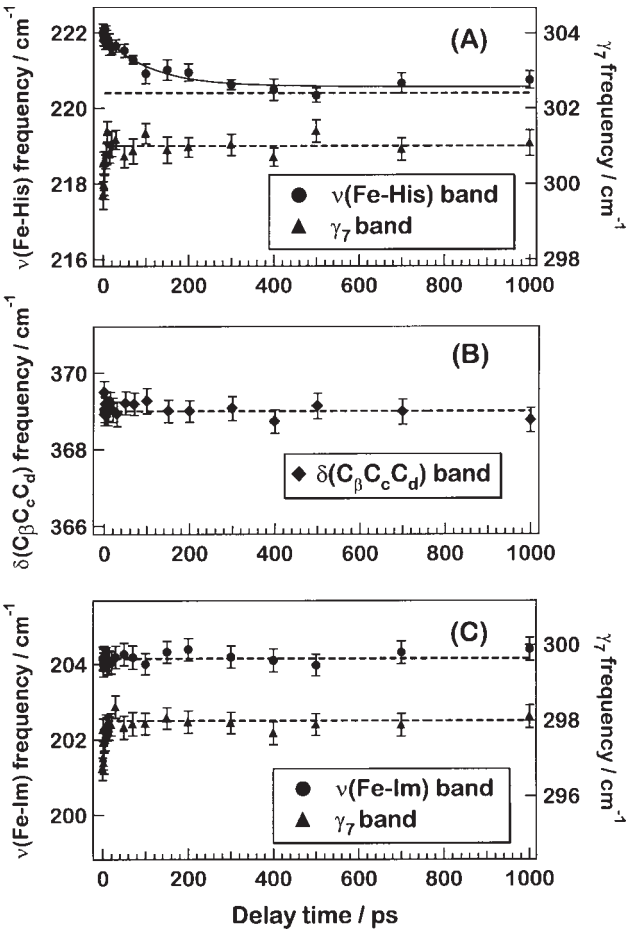

Fig. 8. Temporal changes of the Raman frequencies of some Stokes Raman bands in the low-frequency region. (A) The time dependence of the position of the Stokes ν(Fe-His) (circles) and γ_7 (triangles) bands of photodissociated MbCO. The temporal shift of the ν(Fe-His) band was fitted using a single exponential function, yielding time constants of 106 ± 14 ps (solid line). (B) The time dependence of the position of the Stokes $\delta(C_\beta C_c C_d)$ band (diamonds) of photodissociated MbCO. (C) The time dependence of the position of the Stokes ν(Fe-Im) (circles) and γ_7 (triangles) bands of the photoproduct of the CO-bound (Fe^{II}PPIX)-2MeIm complex. The band positions were obtained as the first moment of the observed bands. The broken lines show the band positions of the equilibrium deligated form (i.e., the deoxy form).

with the equilibrium species, each of the T and R states has a frequency range: 216 to 222 cm^{-1} and 222 to 232 cm^{-1} for the photodissociated T and R preparations (≤10 ns), respectively. For Hb, the difference in the ν(Fe-His) frequencies of the T and R forms was attributed to a difference in the azimuthal angle.[48] Recently, Peterson et al. measured the ν(Fe-His) frequencies of several mutants of sperm whale Mb and examined a correlation between the ν(Fe-His) frequency and heme proximal-His geometry.[64] They attributed changes in the ν(Fe-His) frequency to changes in the azimuthal angle of the His imidazole ring driven by a change in steric factors. However, a

deoxyMb/MbCO comparison of the crystallographic data indicated that the azimuthal angle does not change in Mb as described above.[49,50] If the frequency shift originated from a change in the iron out-of-plane displacement and/or the histidine tilt angle, the shift would accompany an appreciable intensity change in the ν(Fe-His) RR band. Figure 6 shows, however, that there is no change in ν(Fe-His) intensity in the 100-ps time range. Therefore, it is unlikely that the observed frequency shift of the ν(Fe-His) mode is caused by a change of these structural parameters.

Changes in the basicity of an imidazole ring of His residue are known to change the frequency of the ν(Fe-His) mode.[46] An extreme example is found in cytochrome *c* peroxidase (CCP),[65] in which the carboxyl group of Asp235 is hydrogen-bonded to the proximal His at $N_\delta H$. The ν(Fe-His) band in CCP contains two components: one at 233 cm^{-1}, assigned to a conformation with a very strong hydrogen bond to the $N_\delta H$ on the imidazole ring, and the other at 246 cm^{-1}, assigned to a conformation in which a complete proton transfer from the imidazole to the Asp carboxylate group has occurred. The changes in the iron out-of-plane displacement and/or the histidine tilt and azimuthal angles result in a change in the coupling of the Fe-N_{His} mode to the π_{por}-π^*_{por} transition via the orbital mixing of π^*_{por} with $\sigma^*_{Fe\text{-}NHis}$, thereby appreciably changing ν(Fe-His) intensity. However, the change in the hydrogen bond gives rise to a change in the extent of the $\sigma^*_{Fe\text{-}NHis} \rightarrow \pi^*_{por}$ electron donation, and would hardly affect the orbital mixing of π^*_{por} with $\sigma^*_{Fe\text{-}NHis}$. Therefore, the change in the hydrogen bond does not necessarily accompany a change in the ν(Fe-His) Raman intensity. In fact, the N_δ proton of His93 is hydrogen-bonded to the backbone carbonyl of Leu89 and also to the O_γ atom of Ser92. Accordingly, the most probable origin of the ν(Fe-His) downshift of the photodissociated Mb is a change in the hydrogen bond of the proximal His to its surrounding residues.

Structural Changes of the Heme Pocket

The carboxylate group of the heme-7-propionate is hydrogen-bonded to the His97 imidazole ring and the hydroxyl group of Ser92. The frequency of the $\delta(C_\beta C_c C_d)$ band correlates with the status of the hydrogen bond to the propionates in the proximal heme pocket. If the propionates are a part of hydrogen bonds with other residues in the pocket, as in Mb and dimeric Hb from the blood clam *Scaphrca inaequivalvis*,[66] the $\delta(C_\beta C_c C_d)$ mode tends to appear at higher frequencies; but if the propionates are solvent-exposed, as in human Hb, this frequency decreases. In addition, the frequency in a given protein increases as the number of hydrogen bonds to the propionates increases, although there is no fixed relationship between a given frequency and the number of hydrogen bonds. Unlike the ν(Fe-His) band, the $\delta(C_\beta C_c C_d)$ band did not exhibit any frequency shift [Fig. 8(B)], although the $\delta(C_\beta C_c C_d)$ band for the CO-bound form appears at a position 9 cm^{-1} higher than that for the deoxy form. This result suggests that the change in a hydrogen bond of the propionates upon CO dissociation is small and/or takes place within the instrument response time.

Structural Relaxations Probed with Different Techniques

Several experiments have been performed to study the protein response upon CO dissociation, and their results indicated that the protein motion of Mb spans on different time scales. The differences among all of the measurements may be due to the differences in what was probed. Miller and his coworkers found, with femtosecond heterodyne-detected four-wave-mixing measurements, that protein effectively changed its global shape within 500 fs.[67] The observed fast response is consistent with a collective motion mechanism, in which a protein vibration along the reaction coordinate is directly excited by photodissociation of CO. Picosecond time-resolved IR (TRIR) spectroscopy on the amide I band of MbCO indicated that the conformation change of a polypeptide skeleton occurs in a 6 to 8-ps time scale.[68] Therefore, changes in the tertiary structure probed by transient grating or picosecond TRIR spectroscopy do not affect the ν(Fe-His) mode. In contrast, Xie and Simon reported that relaxation of the transient circular dichroism (CD) signal of the N band (probed at 355 nm) of the photodissociated MbCO to the equilibrium deoxy spectrum requires 300 ps.[69] They attributed the CD change to a change in the orientations of the transition dipole moments of the heme relative to those of the aromatic side chains located closely to the heme. The observed temporal behavior of the ν(Fe-His) frequency resembles that of the transient CD signal. The transient absorption measurements of band III showed a highly nonexponential relaxation to its equilibrium position with time constants of 3.5, 83, and 3300 ps.[70] The time constant of the second phase is close to that of the ν(Fe-His) downshift. The latter two experiments probed relatively local changes of protein, that is, changes in the proximal heme pocket. Therefore, there may be relatively slow structural rearrangements around the heme, including a change in hydrogen bonding and the orientational changes of aromatic side chains in the proximal heme pocket.

Vibrational Energy Relaxation[71]

Anti-Stokes Intensities of the Heme Modes

Anti-Stokes Raman intensity is expected to be the most direct probe of the extent and dissipation rate of excess vibrational energy. Figure 9 shows an example of the anti-Stokes TR^3 spectrum of the photodissociated Mb. Spectra A, B, and C are a probe-with-photolysis spectrum at a 1-ps delay, probe-with-

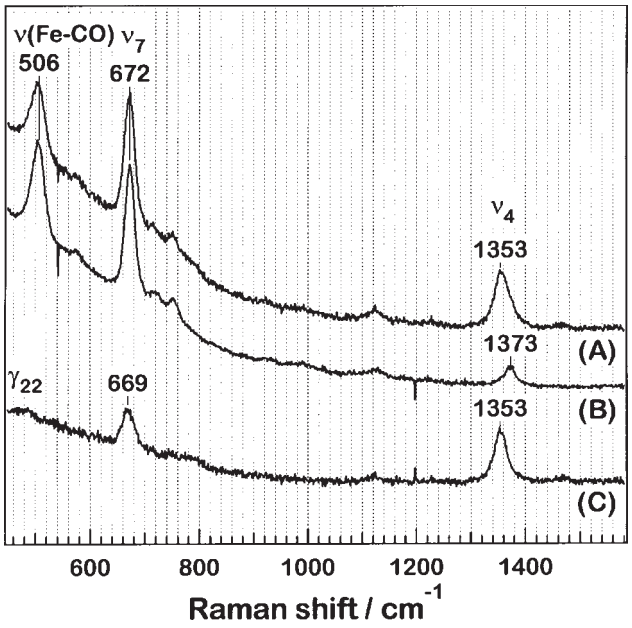

Fig. 9. Anti-Stokes spectra obtained in measurements of an MbCO sample. Spectra A, B, and C represent "probe-with-photolysis" spectrum at a 1-ps delay, "probe-without-photolysis" spectrum, and difference spectrum between A and B (see text for the subtraction procedure), respectively. Note that there is no Raman intensity at the ν_4 frequency of photodissociated Mb in spectrum B. Also note that there is no Raman intensity for the iron-CO stretching mode [ν(Fe-CO)] in spectrum C. The weak band around 490 cm^{-1} in C is due to γ_{22}.

out-photolysis spectrum, and the difference spectrum between A and B, respectively. Note that the ν_4 band in spectrum B gives the contribution from only the CO-bound form and no intensity at the frequency of photodissociated species. This indicates that the probe pulse is weak enough to prevent multiple interactions (i.e., absorption and Raman scattering) by a single heme over the duration of the probe pulse. Because the photon flux becomes high for picosecond pulses in a given average power, it is very important to use weak probe power. With a high photon flux, the ν_4 band appeared for only the photodissociated form in a probe – without – photolysis spectrum, indicating that there is a significant probability for the heme to be photoexcited and provide Raman scattering within a single probe pulse. Because the quantum efficiency of the CO photodissociation is near unity, the complete absence of the Raman band belonging to the photodissociated form in the spectrum without photolysis corroborates the adoption of a proper experimental condition for the probe power. The anti-Stokes TR^3 difference spectra between –5 and 50 ps are shown in Figure 10. Anti-Stokes intensities were highest at a 1 ps delay, when the ν_3, ν_4, ν_5, ν_6, and ν_7 bands were observed at 1469, 1353, 1118, 783, and 669 cm^{-1}, respectively. These bands lost intensity as the delay time increased, and reached their equilibrium intensities at a 10 ps delay.

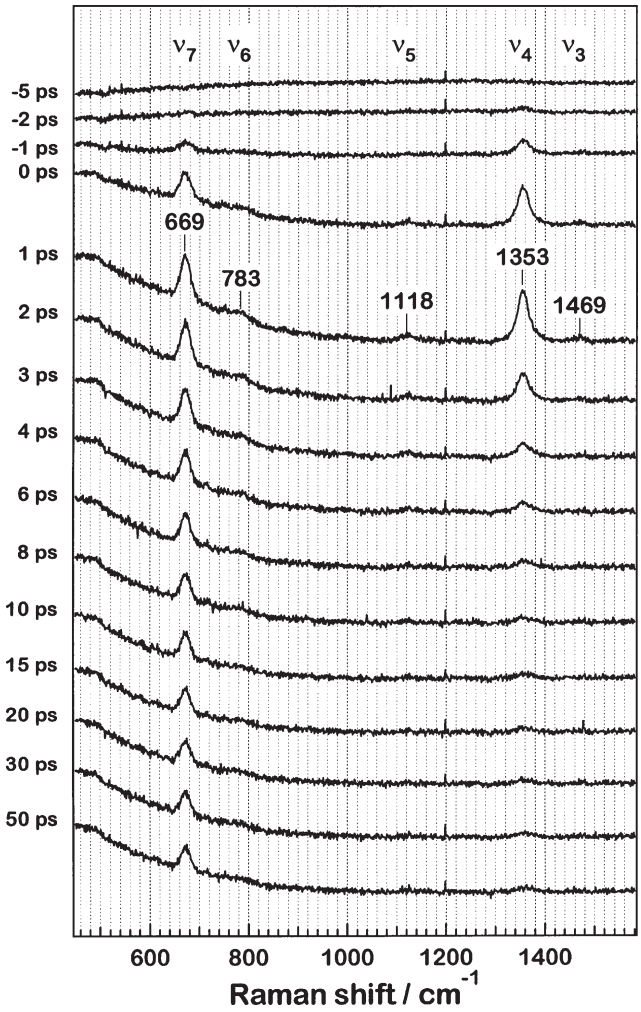

Fig. 10. TR^3 anti-Stokes spectra of photodissociated MbCO in the 450 to 1600-cm^{-1} region.

Figure 11 shows the temporal changes of anti-Stokes ν_4 and ν_7 band intensities. The anti-Stokes intensity develops within the instrument response time. This is consistent with the photodissociation of CO from the heme, which takes place within 50 fs.[14] The instrument response was deconvoluted from the decay of the anti-Stokes intensity using a Gaussian fit to the cross correlation signal. This analysis obtained the decay constants of 1.1 ± 0.6 ps for the ν_4 band and 1.9 ± 0.6 ps for the ν_7 band. Because there is no intensity change in the Stokes ν_4 and ν_7 bands in the 3 to 50-ps time range, the observed intensity decay in the anti-Stokes ν_4 and ν_7 bands can be ascribed to vibrational energy relaxation.

Figure 12 delineates the detailed spectral change of the Stokes ν_4 band after photodissociation. At a delay of 1 ps, the center of the ν_4 band is located at 1352 cm^{-1}, and the band is broadened with a full width at half maximum (FWHM) of 19.7 ± 0.6 cm^{-1}. The band shifts to 1355 cm^{-1} and becomes

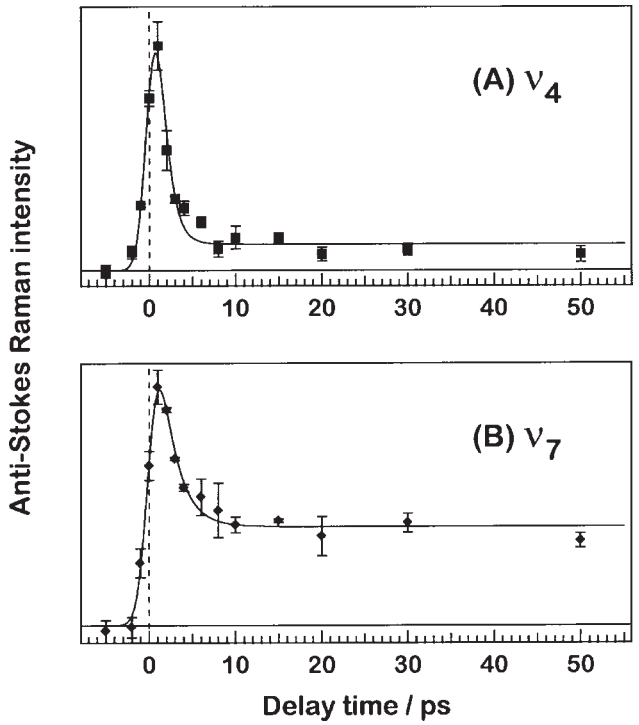

Fig. 11. Temporal changes of the Raman intensity of the anti-Stokes ν_4 (A) and ν_7 bands (B) of photodissociated MbCO. The solid lines are fit using an exponential function of the form $A[\exp(-t/\tau_{decay}) + B]$ (an instantaneous rise and an exponential decay) convoluted with an instrument function as shown in the caption of Figure 5. The lines shown in this figure were obtained with the parameters of $\tau_{decay} = 1.1 \pm 0.6$ ps and $B = 0.03 \pm 0.01$ for the ν_4 band, and $\tau_{decay} = 1.9 \pm 0.6$ ps and $B = 0.31 \pm 0.02$ for the ν_7 band.

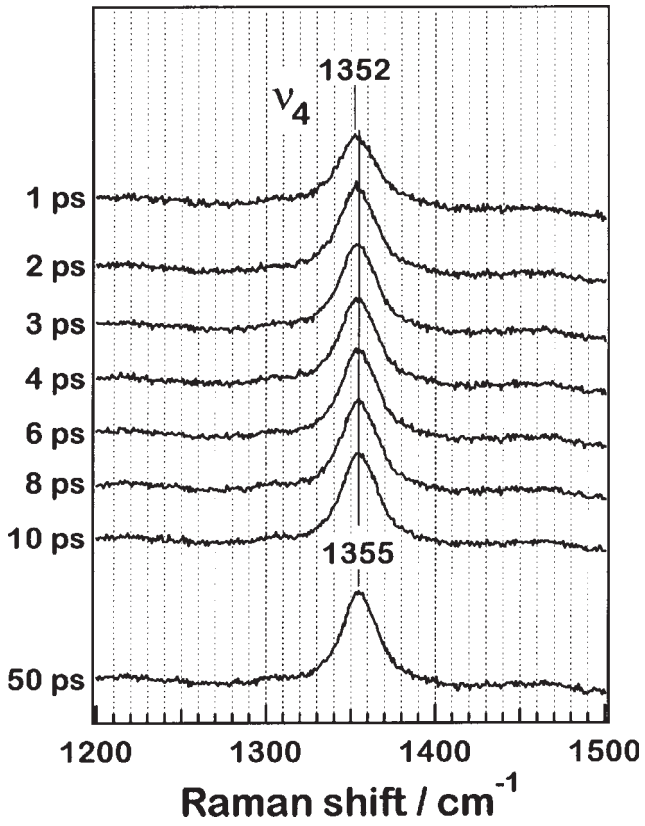

Fig. 12. Closeup of TR[3] Stokes spectra in the ν_4 region.

narrower (FWHM = 17.4 ± 0.6 cm^{-1}) at a 50-ps delay. Similar trends are observed for the ν_7 band, which is centered at 669 cm^{-1} and is broadened (FWHM = 22.7 ± 0.7 cm^{-1}) for a 1-ps delay, but is shifted to 671 cm^{-1} and becomes narrower (FWHM = 19.7 ± 0.7 cm^{-1}) for a 50-ps delay. Recently, similar features were also observed for nickel octaethylporphyrin in benzene.[72]

Heme Cooling

A 540-nm photon excites the heme into the π_{por}-π^*_{por} state [^{1}Q(1, 0)], thereby depositing 221 kJ/mol of energy. The π_{por}-π^*_{por}-excited heme is believed to relax to a level having the antibonding character of the Fe-CO bond, although its energy level is presently unclear. The absorbed photon energy is significantly higher than the energy required to break the Fe-CO bond, and therefore, excess energy is deposited on the photolyzed heme. The enthalpy difference between Mb + CO (gas) and MbCO is approximately 90 kJ/mol,[73] so the heme and CO share approximately 130 kJ/mol of excess energy. Partitioning of this excess energy depends on its mechanism. If the $^5T_2$ or $^3T_1$ state of Fe^{II} were involved, as was suggested for hemoglobin-CO (HbCO),[13] the heme would possess an excess energy of between 50 and 100 kJ/mol immediately after photodissociation.

Pioneering work on the energy flow from the heme into the protein matrix was reported by Henry et al.,[28] who carried out molecular dynamics simulations for Mb and cytochrome *c* with initial energy deposits corresponding to optical excitation at both 532 and 355 nm. The simulation predicted a fast initial relaxation phase with decay constants of between 1 and 4 ps, followed by a slower relaxation phase with decay constants of between 20 and 40 ps. To compare those predictions with the results in this work, it is necessary to estimate the temperature decay rate of the heme. The anti-Stokes/Stokes Raman intensity ratio is determined by the Boltzmann factor for the vibrational mode in question, assuming a statistical distribution of vibrational energy. When the observed kinetics of population decay in vibrationally excited states are converted to temperatures by assuming a Boltzmann distribution, the time constants of 1.1 ± 0.6 (ν_4) and 1.9 ± 0.6 ps (ν_7) for the population decay give rise to time constants of about 2 ps for the temperature decay. This value appears to be close to the value of the fast component predicted by Henry et al.[28] However, the molecular dynamics simulations suggested a ratio of 50:50 for

the magnitudes of the fast and the slow components, whereas we did not observe such a large contribution of the slow component in Figure 10. It is noted that the simulation was conducted *in vacuo* and neglected the effect of the water bath, which works as an extensive thermal sink. In fact, fast heating of water with a time constant of 7.5 ± 2.0 ps was observed for Mb in D_2O.[74] Genberg et al. studied the vibrational energy relaxation of optically excited hemeproteins by using a transient phase grating technique, and they found that vibrational energy was transferred from the heme to the water interface through the protein matrix in less than 20 ps.[75] A molecular dynamics simulation with the presence of water molecules indicated that the inclusion of water increases the rate of cooling to a 10-ps time scale.[76] Disregarding the effect of the water bath may decelerate the cooling rate of heme, resulting in a larger contribution by the slow component.

Hopkins and his coworkers measured the TR^3 spectra of deoxyHb with a time resolution of 8 ps.[77] Intensity changes of both negative transients in Stokes and positive transients in anti-Stokes showed population changes with a time constant of between 2 and 5 ps, to which the 1 to 2-ps decay of Figure 10 obtained with a higher time resolution is comparable, despite differences in the globin (Mb vs. Hb) and phenomena (CO-photodissociation vs. electronic excitation). Petrich et al. studied the vibrational relaxation of hemeproteins indirectly using femtosecond Stokes resonance Raman spectroscopy, and they estimated the temperature of heme in HbCO based on the band shift of the ν_4 mode.[78] They concluded that the heme in the HbCO photoproduct was substantially cooled within 10 ps. Li et al. qualitatively analyzed Stokes and anti-Stokes Raman scattering of different hemeproteins to determine the heme vibrational temperature as a function of nanosecond laser flux. They obtained a time constant of about 4 ps for heme cooling.[41] These experimental results on the time scale of vibrational energy relaxation are in agreement with the results in this work.

The fast energy dissipation from the globin to the water bath has also been noted in femtosecond TRIR studies that monitor the heating of water caused by the photoexcitation of deoxyMb.[74] The observed kinetics was fitted with a model having two time constants. The fast component was best fitted by a Gaussian rise function with a time constant of 7.5 ± 1.5 ps, and the slow component was described by a time constant of about 20 ps with 40% of the total amplitude. A comparison of the heme cooling (TR^3) and water heating (TRIR) studies suggests that there are two channels of energy dissipation from the protein to the water bath. One is a classical diffusion process, and it is responsible for the slow component; the observed time constant is in reasonable agreement with that calculated using the classical diffusion theory. The other is through the collective motions of the protein,[74] and it is responsible for the fast component. The time constant of heme cooling (3 ps) is shorter than that of water heating (7.5 ps). This time lag may correspond to the time required for energy propagation via the collective low-frequency modes of the protein. Very recently, Sagnella et al. proposed that a possible doorway for energy release from the vibrationally excited heme involves the interaction of its propionate groups with neighboring solvent molecules.[79]

Vibrational Relaxation of the CO Stretching Mode

One-[80] and two-color[81] infrared pump-infrared probe spectroscopy has been used to determine the vibrational relaxation time (T_1) for the CO stretching vibrations in the unphotolyzed state of MbCO in D_2O at 300 K. Both measurements obtained similar results of 17 ps for T_1 time. The CO T_1 time can be affected by the protein structure[80]: two different conformers of MbCO have significantly different T_1 times. It is interesting to compare the time constants of the vibrational energy relaxations of the heme modes with that of the internal mode of CO bound to the heme. The T_1 of the CO stretch is much longer than the time constants observed for heme cooling in Mb, indicating that there is not efficient intramolecular energy exchange between the bound CO and the porphyrin ring. Recent studies demonstrated that the inter- and intramolecular processes of vibrational relaxation must be considered to be in competition even for large molecules such as *trans*-stilbene[82–87] and metalloporphyrins[72,88–90]. One reason for the less efficient energy exchange is the relatively low frequencies of the other FeCO modes (577 and 512 cm^{-1} for the FeCO bend and FeC stretch of MbCO, respectively). These frequencies imply that at least three quanta are required to come within a few hundred wavenumbers of the energy of the CO stretching mode. A pathway involving the transfer of the CO vibrational energy into other FeCO modes therefore requires large anharmonic coupling.

There are studies on the vibrational energy relaxation of CO in the photolyzed state, where CO is not covalently attached but is trapped within a docking site. The structure and dynamics of the photolyzed state have recently been probed using X-ray diffraction,[91–94] vibrational spectroscopy,[95,96] and computer simulation.[97–99] Photolysis of MbCO produces a significant population of CO in its excited vibrational state. Based on time-resolved mid-IR absorbance measurements, T_1 time of 600 ± 150 ps was determined.[100] Because the photodissociated CO has no covalent interactions, its T_1 time is significantly longer than that observed in the bound state. Measurement of this relaxation time will clarify the role of the "protein solvent" in the relaxation of CO. The Landau-Teller theory predicted that the relaxation rate of $1/T_1$ is expressed remarkably well by the Fourier component of time-dependent friction evaluated at the frequency of the oscillator,[101] which is connected to the time correlation function of the fluctuating force along the vibrational coordinate by the second fluctua-

tion-dissipation theorem. Sagnella et al. computed the influence spectrum, which is the distribution of the square of the coupling constants between the CO stretch and the bath modes as a function of frequency.[100] In their simulations, the relaxation was dominated by short-ranged van der Waals interactions, with the residues forming the inner wall of the heme pocket of Mb. The data suggest that the mechanism for the vibrational relaxation of CO in Mb takes place through successive, noncorrelated collisions with the pocket residues, acting as a first solvation shell to the CO molecule.

Vibrational Relaxation of the Amide I Mode

The exchange mechanism of vibrational energy within proteins is little understood. Several time-resolved experiments were performed with picosecond and femtosecond infrared pulses to study the dissipation of locally deposited energy in the protein backbone (amide I mode).[102–104] The amide I vibrational mode involves mainly the C=O stretching motion of the peptide backbone under a small amount of mixing with the CN and NH motions.[105] Because the amide I vibrational mode is a strong infrared absorber, this band is ideal for mid-infrared transient absorption ("pump-probe") measurements. Mb is almost entirely α-helical in the secondary structure, and it shows the amide I band centered near 1650 cm^{-1} in D_2O. Peterson et al. carried out mid-infrared transient absorption measurements on the amide I band of Mb in a wide temperature range (6 to 310 K).[103] The temperature dependence of the vibrational relaxation in the solvent mixture is slight, changing from 1.9 ± 0.2 ps below 100 K to 1.2 ± 0.2 ps at 310 K. Tokmakoff et al.[106] and Kenkre et al.[107] gave detailed discussions on the temperature dependencies of vibrational relaxation. In general, if two or more low-frequency bath modes are involved, vibrational relaxation has a significant temperature dependence, because at higher temperatures, the thermal population of the bath modes increase the relaxation rate through a stimulated process. The lack of a strong temperature dependence is indicative of a low-order relaxation process where energy is transferred into the high-energy modes of the system rather than directly to the low-energy solvent or protein "bath" modes. Femtosecond pump-probe measurements by Hamm et al. on small proteins, including apamin, scyllatoxin, and bovine pancreatic tripsin inhibitor, each of which contains both of the α-helix and β-sheet structures in different proportions, show an identical lifetime of 1.2 ps for amide I.[102] Despite the differences in their sizes and secondary structures, the amide I relaxation dynamics observed in both of these studies are essentially the same and appear to be fundamental features of the amide I mode in polypeptides and proteins. It is interesting that the heme and the amide I modes show similar vibrational lifetimes,[104] although the coincidence may be accidental.

Summary and Prospects

Mb looks like a "hydrogen molecule" for physicochemical studies on protein dynamics. Many kinds of spectroscopic techniques, including ultrafast spectroscopy, have been applied to study the dynamic properties of this protein, as described above. It became apparent from these studies on the heme that the structural change of the heme ring is completed within 1 ps after CO photodissociation. At the same time, large amounts of excess vibrational energy are selectively deposited at the heme site. As described in the section on "Vibrational Energy Relaxation," the mechanism of vibrational energy transfer within proteins has not been extensively studied thus far because of a lack of an appropriate method. Raman bands of some aromatic side chains, such as tryptophan, tyrosine, and phenylalanin residues, are resonantly enhanced with UV probe light.[108] The anti-Stokes scattering of these residues serve as a good probe of the extent of the vibrational excess energy at their locations in proteins. If such measurements are accomplished, the vibrational energy transfer from the heme to the surrounding protein, and from the protein to water, can be followed using ultrafast spectroscopic methods to provide spatial mapping of the vibrational energy relaxation pathways. Detailed structural information on these systems facilitates the construction of conceptual models on the vibrational energy exchange and also a detailed theoretical modeling of the process. Thus, hemeproteins provide ideal model systems for understanding vibrational energy relaxation not only in protein but also in general condensed phases.

The ultrafast structural change at the heme site perturbs the protein structure in a step-function manner. Therefore, photodissociation of CO in Mb provides a good opportunity to study the protein response function for the reaction at the heme. In this study, the protein response was observed as the frequency shift of the ν(Fe-His) mode with the 100-ps time constant. Although the response function is expected to be far from simple, one can consider two limiting cases with respect to the length scale and dynamics of the protein response function for the reaction at the heme site. On a long time scale for the motions, atomic displacements should be considered diffusive in nature. The protein motion between local minima in its structure is averaged over a certain time interval, and the net atomic displacements along the reaction coordinate appear as a thermally activated Brownian process. The length of any given relaxation component in this particular scenario can be on the order of a single amino acid residue (i.e., localized motions). An interconversion between the so-called "open" and "closed" forms is a typical example.[109] A large number of nearly degenerate conformational substates leads to a distribution of barrier heights and pathways so that the structural relaxation is highly nonexponential, as observed in the geminate recombination of CO[110, 111] and other ligands.[112,113] Because proteins

have a highly associated nature, this part of the protein response function is often modeled as analogous to glass relaxation dynamics.[114] At the other extreme, in the short-time dynamics of the protein response to the reaction forces, the dominant contribution to the protein displacements can involve nondiffusive motions. In this limit, the reaction forces are redistributed over the entire protein structure. The nascent potential energy gradients that develop during ligand dissociation would lead to the collective displacement of a large number of atoms. In this event, the propagation of the structural changes would best be described as the displacement of atoms in a superposition of the low-frequency collective modes of the protein. The validity of the description is the same as the justification for the modal treatment (e.g., instantaneous-normal mode approach) that models the short-time behavior of liquids such as inertial motions.[115,116] For proteins, the atoms are covalently bonded, and the overall correlation length scale is determined by forces much stronger than the intermolecular forces in liquids. The use of a modal description for the short-time dynamics of protein motions is more rigorous than it is for liquids. Normal mode analysis by Seno and Go found that 57% of the tertiary structural changes can be accounted for by the displacements of six spatially extended modes with frequencies ranging from 5 to 12 cm^{-1}.[117] Finally, it should be pointed out that the validity of the modal description is connected to vibrational energy relaxation in the protein. The time scale of energy relaxation forms the guidelines for considering whether protein motions are collective or diffusive. For example, if the protein modes are strongly anharmonically coupled, intramolecular vibrational redistribution within the protein can occur very rapidly, which can then result in ultrafast exponential initial relaxation. This is a general argument for stochastic processes in a condensed phase.[118,119]

Thus, there are strong connections between the protein dynamics and condensed-phase dynamics involving chemical reactions. Moreover, proteins are the media of which static structures are often determined at atomic resolution with X-ray crystallography and NMR spectroscopy. The structures in nature can be modified artificially using site-directed mutation techniques. These features are distinct advantages in physicochemical studies on proteins compared to such studies on liquids. Therefore, biological questions, besides being important to address in their own right, present a relatively untapped fertile source stimulating studies of physical chemistry in condensed phases. For this reason, the most detailed understanding of condensed-phase reaction dynamics may come from studies of biological systems. In oxygen binding by Hb, for example, the central molecule (the heme) and the environment (the globin) profoundly affect each other in a beautiful manner: the protein's structural changes form a strongly coupled system in which tertiary relaxation is cascaded into the quaternary structural transition. The biomechanics of the tertiary structural changes in Mb are important for a detailed understanding of functionary important protein motions and cooperative oxygen-binding in Hb. Once the dominant mechanism for the tertiary structural changes is clarified, the molecular mechanism behind the R to T quaternary structural changes and general allosteric effects may become clear. Combined advances in theoretical and experimental methods involving studies over a broad range of time scales and length scales for the protein response are required to reach this ultimate goal.

The authors thank Dr. Yuki Uesugi for her contribution to the development of our picosecond time-resolved resonance Raman apparatus. Stimulating discussions with Prof. Paul M. Champion of Northeastern University and with Prof. Robin M. Hochstrasser of the University of Pennsylvania are gratefully acknowledged. This research was supported in part by a Grant-in-Aid for Scientific Research on Priority Area (No. 12045264) given to T.K. from the Ministry of Education, Science, Sports and Culture, Japan, and by a Grant-in-Aid for Encouragement Young Scientists (No. 11740339) given to Y.M. from the Japan Society for the Promotion of Science.

REFERENCES

[1] McCammon, J. A.; Harvey, S. C. Dynamics of Proteins and Nucleic Acids; Cambridge University Press: Cambridge, 1987.
[2] Brooks, C. L., III; Karplus, M.; Pettit, B. M. Proteins: A Theoretical Perspective of Dynamics, Structure, and Thermodynamics; Wiley: New York, 1988.
[3] Hochstrasser, R. M. J Chem Educ 1998, 75, 559.
[4] Elsaesser, T.; Kaiser, W. Ann Rev Phys Chem 1991, 42, 83.
[5] Seilmeier, A.; Kaiser, W. In Ultrashort Laser Pulses, Generation and Applications, Vol 60; Kaiser, W., Ed.; Springer-Verlag: Berlin, 1993; p. 279.
[6] Owrutsky, J. C.; Raftery, D.; Hochstrasser, R. M. Ann Rev Phys Chem 1994, 45, 519.
[7] Joo, T.; Jia, Y.; Yu, J.-Y.; Jonas, D. M.; Fleming, G. R. J Phys Chem 1996, 100, 2399.
[8] Leeson, D. T.; Wiersma, D. A.; Fritsch, K.; Friedrich, J. J Phys. Chem B 1997, 101, 6331.
[9] Lim, M.; Hamm, P.; Hochstrasser, R. M. Proc Natl Acad Sci USA 1998, 95, 15315.
[10] Shibata, Y.; Kurita, A.; Kushida, T. Biochemistry 1999, 38, 1789.
[11] Dickerson, R. E.; Geiss, I. Hemoglobin: Structure, Function, Evolution, and Pathology; Benjamin Cummings: Menlo Park, 1983.
[12] Gibson, Q. H. J Physiol 1956, 134, 112.
[13] Greene, B. I.; Hochstrasser, R. M.; Weisman, R. B.; Eaton, W. A. Proc Natl Acad Sci USA 1978, 75, 5255.

[14] Petrich, J. W.; Poyart, C.; Martin, J. L. Biochemistry 1988, 27, 4049.
[15] Gibson, Q. H.; Olson, J. S.; McKinnie, R. E.; Rohlfs, R. J. J Biol Chem 1986, 261, 10228.
[16] Kachalova, G. S.; Pepov, A. N.; Bartunik, H. D. Science 1999, 284, 473.
[17] Spiro, T. G., Ed. Biological Applications of Raman Spectroscopy; Wiley: New York, 1987.
[18] Wynne, K.; Hochstrasser, R. M. Chem Phys 1995, 193, 211.
[19] Hamm, P. Chem Phys 1995, 200, 415.
[20] Hamm, P.; Wiemann, S.; Zurek, M.; Zinth, W. Opt Lett 1994, 19, 1642.
[21] Hamm, P.; Lim, M.; Hochstrasser, R. M. J Chem Phys 1997, 107, 10523.
[22] Okamoto, H.; Tasumi, M. Chem Phys Lett 1996, 256, 502.
[23] Okamoto, H. Chem Phys Lett 1998, 283, 33.
[24] Akhremitchev, B. B.; Wang, C.; Walker, G. C. Rev Sci Inst 1996, 67, 3799.
[25] Schomacker, K. T.; Bangcharoenpaurpong, O.; Champion, P. M. J Chem Phys 1984, 80, 4701.
[26] Okamoto, H.; Nakabayashi, T.; Tasumi, M. J Phys Chem A 1997, 101, 3488.
[27] Shreve, A. P.; Mathies, R. A. J Phys Chem 1995, 99, 7285.
[28] Henry, E. R.; Eaton, W. A.; Hochstrasser, R. M. Proc Natl Acad Sci USA 1986, 83, 8982.
[29] Horng, M. L.; Gardecki, J. A.; Papazyan, A.; Maroncelli, M. J Phys Chem 1995, 99, 17311.
[30] Uesugi, Y.; Mizutani, Y.; Kitagawa, T. Rev Sci Instrum 1997, 68, 4001.
[31] Uesugi, Y.; Mizutani, Y.; Kruglik, S. G.; Shvedko, A. G.; Orlovich, V. A.; Kitagawa, T. J Raman Spectrosc 2000, 31, 339.
[32] Hamaguchi, H.; Gustafson, T. L. Ann Rev Phys Chem 1994, 45, 593, and references therein.
[33] Kaminaka, S.; Kitagawa, T. Appl Spectrosc 1995, 49, 685.
[34] Mizutani, Y. J Chem Phys 1998, 109, 9197.
[35] Mizutani, Y.; Kitagawa, T. Manuscript in preparation.
[36] Abe, M.; Kitagawa, T.; Kyogoku, Y. J Chem Phys 1978, 69, 4526.
[37] Li, X.-Y.; Czernucszewicz, R. S.; Kincaid, J. R.; Stein, P.; Spiro, T. G. J Phys Chem 1990, 94, 47.
[38] Lim, M.; Jackson, T. A.; Anfinrud, P. A. J Phys Chem 1996, 100, 12043.
[39] Petrich, J. W.; Martin, J. L. Chem Phys 1989, 131, 31.
[40] Cornelius, P. A.; Steele, A. W.; Chernoff, D. A.; Hochstrasser, R.M. Proc Natl Acad Sci USA 1981, 78, 7526.
[41] Li, P.; Sage, J. T.; Champion, P. M. J Chem Phys 1992, 97, 3214.
[42] Rosca, F.; Kumar, A. T. N.; Ye, X.; Sjodin, T.; Demidov, A. A.; Champion, P. M. J Phys Chem A 2000, 104, 4280.
[43] Gibson, Q. H.; Olson, J. S.; McKinnie, R. E.; Rohlfs, R. J. J Biol Chem 1986, 261, 10228.
[44] Kitagawa, T.; Nagai, K.; Tsubaki, M. FEBS Lett 1979, 104, 376.
[45] Hu, S.; Smith, K. M.; Spiro, T. G. J Am Chem Soc 1996, 118, 12638.
[46] Kitagawa, T. In Biological Applications of Raman Spectroscopy, Vol. III; Spiro, T. G., Ed.; Wiley: New York, 1987; p 97.
[47] Rousseau, D. L.; Friedman, J. M. In Biological Applications of Raman Spectroscopy, Vol. III; Spiro, T. G., Ed.; Wiley: New York, 1987; p 133.
[48] Bangcharoenpaurpong, O.; Schomacker, K. T.; Champion, P. M. J Am Chem Soc 1984, 106, 5688.
[49] Takano, T. J Mol Biol 1977, 110, 569.
[50] Takano, T. J Mol Biol 1977, 110, 537.
[51] Kuczera, K.; Lambry, J.-C.; Martin, J.-L.; Karplus, M. Proc Natl Acad Sci USA 1993, 90, 5805.
[52] Lim, M.; Jackson, T. A.; Anfinrud, P. A. Proc Natl Acad Sci USA 1993, 90, 5801.
[53] Schaad, O.; Zhou, H.-X.; Szabo, A.; Eaton, W. A.; Henry, E. R. Proc Natl Acad Sci USA 1993, 90, 9547.
[54] Li, H.; Elber, R.; Straub, J. E. J Biol Chem 1993, 268, 17908.
[55] Findsen, E. W.; Scott, T. W.; Chance, M. R.; Friedman, J. M. J Am Chem Soc 1985, 107, 3355.
[56] Nagai, K.; Kitagawa, T. Proc Natl Acad Sci USA 1980, 77, 2033.
[57] Nagai, K.; Kitagawa, T.; Morimoto, H. J Mol Biol 1980, 136, 271.
[58] Ondrias, M. R.; Rousseau, D. L.; Shelnutt, J. A.; Simon, S. R. Biochemistry 1985, 21, 3428.
[59] Friedman, J. M.; Rousseau, D. L.; Ondrias, M. R.; Stepnoski, R. A. Science 1982, 218, 1244.
[60] Friedman, J. M.; Stepnoski, R. A.; Nobel, R. W. FEBS Lett 1982, 146, 278.
[61] Friedman, J. M.; Rousseau, D. L.; Ondrias, M. R. Ann Rev Phys Chem 1982, 33, 471.
[62] Irwin, M. J.; Atkinson, G. H. Nature (London) 1981, 293, 317.
[63] Stein, P.; Terner, J.; Spiro, T. G. J Phys Chem 1982, 86, 168.
[64] Peterson, E. S.; Friedman, J. M.; Chien, E. Y. T.; Sliger, S. G. Biochemistry 1998, 37, 12301.
[65] Smulevich, G.; Mauro, J. M.; Fishel, L. A.; English, A. M.; Kraut, J.; Spiro, T. G. Biochemistry 1988, 27, 5477.
[66] Royer, W. E., Jr. J Mol Biol 1994, 235, 657.
[67] Goodno, G. D.; Astinov, V.; Miller, R. J. D. J Phys Chem A 1999, 103, 10630.
[68] Causgrove, T. P.; Dyer, R. B. J Phys Chem 1996, 100, 3273.
[69] Xie, X.; Simon, J. D. Biochemistry 1991, 30, 3682.
[70] Jackson, T. A.; Lim, M.; Anfinrud, P. A. J Chem Phys 1994, 180, 131.
[71] Mizutani, Y.; Kitagawa, T. Science 1997, 278, 443.
[72] Mizutani, Y.; Uesugi, Y.; Kitagawa, T. J Chem Phys 1999, 111, 8950.
[73] Keyes, M. H.; Falley, M.; Lumry, R. J Am Chem Soc 1971, 93, 2035.
[74] Lian, T.; Locke, B.; Kholodenko, Y.; Hochstrasser, R. M. J Phys Chem 1994, 98, 11648.
[75] Genberg, L.; Heisel, F.; McLendon, G.; Miller, R. J. D. J Phys Chem 1987, 91, 5521.
[76] Miller, R. J. D. Ann Rev Phys Chem 1994, 42, 581.
[77] Lingle, R., Jr.; Xu, X.; Zhu, H.; Yu, S.-C.; Hopkins, J. B. J Phys Chem 1991, 95, 9320.

[78] Petrich, J. W.; Martin, J. L.; Houde, D.; Poyart, C.; Orszag, A. Biochemistry 1987, 26, 7914.
[79] Sagnella, D. E.; Straub, J. E.; Thirumalai, D. J Chem Phys 2000, 113, 7702.
[80] Hill, J. R.; Tokmakoff, A.; Peterson, K. A.; Sauter, B.; Zimdars, D.; Dlott, D. D.; Fayer, M. D. J Phys Chem 1994, 98, 11213.
[81] Owrutsky, J. C.; Li, M.; Locke, B.; Hochstrasser, R. M. J Phys Chem 1995, 99, 4842.
[82] Sension, R. J.; Szarka, A. Z.; Hochstrasser, R. M. J Chem Phys 1992, 97, 5239.
[83] Sension, R. J.; Repinec, S. T.; Szarka, A. Z.; Hochstrasser, R. M. J Chem Phys 1993, 98, 6291.
[84] Qian, J.; Schultz, S. L.; Jean, J. M. Chem Phys Lett 1995, 233, 9.
[85] Schultz, S. L.; Qian, J.; Jean, J. M. J Phys Chem A 1997, 101, 1000.
[86] Nakabayashi, T.; Okamoto, H.; Tasumi, M. J Phys Chem A 1997, 101, 7189.
[87] Nakabayashi, T.; Okamoto, H.; Tasumi, M. J Phys Chem A 1998, 102, 9686.
[88] Sato, S.; Kitagawa, T. Appl Phys B 1994, 59, 415.
[89] Schneebeck, M. C.; Vigil, L. E.; Ondrias, M. R. Chem Phys Lett 1993, 215, 251.
[90] Simpson, M. C.; Peterson, E. S.; Shannon, C. F.; Eads, D. D.; Friedman, J. M.; Cheatum, C. M.; Ondrias, M. R. J Am Chem Soc 1997, 119, 5110.
[91] Schlichting, I.; Berendzen, J.; Phillips, G. N., Jr.; Sweet, R. M. Nature 1994, 371, 808.
[92] Teng, T. Y.; Srajer, V.; Moffat, K. Nat Struct Biol 1994, 1, 701.
[93] Hartmann, H.; Zimser, S.; Komninos, P.; Scheinder, R. T.; Nienhaus, G. U.; Parak, F. Proc Natl Acad Sci USA 1996, 93, 7013.
[94] Šrajer, V.; Teng, T.; Ursby, T.; Pradervand, C.; Ren, Z.; Adachi, S.; Schildkamp, W.; Bourgeois, D.; Wulff, M.; Moffat, K. Science 1996, 274, 1726.
[95] Lim, M.; Jackson, T. A.; Anfinrud, P. A. Science 1995, 269, 962.
[96] Lim, M.; Jackson, T. A.; Anfinrud, P. A. Nat Struct Biol 1997, 4, 209.
[97] Straub, J. E.; Karplus, M. Chem Phys 1991, 158, 221.
[98] Ma, J.; Huo, S.; Straub, J. E. J Am Chem Soc 1997, 119, 4355.
[99] Vitkup, D.; Petsko, G. A.; Karplus, M. Nat Struct Biol 1997, 4, 202.
[100] Sagnella, D. E.; Straub, J. E.; Jackson, T. A.; Lim, M.; Anfinrud, P. A. Proc Natl Acad Sci USA 1999, 96, 14324.
[101] Whitnell, R. M.; Wilson, K. R.; Hynes, J. T. J Phys Chem 1990, 94, 8625.
[102] Hamm, P.; Lim, M.; Hochstrasser, R. M. J Phys Chem B 1998, 102, 6123.
[103] Peterson, K. A.; Rella, C. W.; Engholm, J. R.; Schwettman, H. A. J Phys Chem B 1999, 103, 557.
[104] Xie, A.; van der Meer, L.; Hoff, W.; Austin, R. H. Phys Rev Lett 2000, 84, 5435.
[105] Miyazawa, T.; Shimanouchi, T.; Mizushima, S. J Chem Phys 1958, 29, 611.
[106] Tokmakoff, A.; Sauter, B.; Feyer, M. D. J Chem Phys 1994, 100, 9035.
[107] Kenkre, V. M.; Tokmakoff, A.; Feyer, M. D. J Chem Phys 1994, 101, 10618.
[108] Harada, I.; Takeuchi, H. In Spectroscopy of Biological Systems, Vol. 13; Clark, R. J. H.; Hester, R. E., Eds.; Wiley: New York, 1986; p 113.
[109] Tian, W. D.; Sage, J. T.; Champion, P. M.; Chien, E.; Sligar, S. G. Biochemistry 1996, 35, 3487.
[110] Lambright, D. G.; Balasubramanian, S.; Boxer, S. G. Biochemistry 1993, 32, 10116.
[111] Tian, W. D.; Sage, J. T.; Šrajer, V.; Champion, P. M. Phys Rev Lett 1992, 68, 408.
[112] Chernoff, D. A.; Hochstrasser, R. M.; Steele, A. W. Proc Natl Acad Sci USA 1980, 77, 5606.
[113] Petrich, J. W.; Lambry, J. C.; Kuczera, K.; Karplus, M.; Poyart, C.; Martin, J. L. Biochemistry 1991, 30, 3975.
[114] Hagen, S. J.; Eaton, W. A. J Chem Phys 1996, 104, 3395.
[115] Bunchner, M.; Ladanyi, B. M.; Stratt, R. M. J Chem Phys 1992, 97, 8522.
[116] Cho, M.; Fleming, G. R.; Saito, S.; Ohmine, I.; Stratt, R. M. J Chem Phys 1994, 100, 6672.
[117] Seno, Y.; Go, N. J Mol Biol 1990, 216, 111.
[118] Kubo, R.; Toda, M.; Hashitsume, N. Statistical Physics II: Nonequilibrium Statistical Mechanics; Springer-Verlag: Berlin, 1991; Chapter 2.
[119] Kubo, R. In Fluctuations, Relaxation, and Resonance in Magnetic Systems; ter Haar, D., Ed.; Plenum Press: New York, 1962; p 23.

